Supplement of Atmos. Chem. Phys., 23, 14393–14424, 2023
https://doi.org/10.5194/acp-23-14393-2023-supplement

Atmospheric Chemistry and Physics
Open Access
EGU

Supplement of

Radical chemistry and ozone production at a UK coastal receptor site

Robert Woodward-Massey et al.

Correspondence to: Lisa K. Whalley (l.k.whalley@leeds.ac.uk) and Dwayne E. Heard (d.e.heard@leeds.ac.uk)

Supplementary Tables S1 to S3.

Table S1. Median trace gas mixing ratios and meteorological parameters, split according to wind direction (NW–SE = <165° and >285°; SW = 180°–270°).

Species or meteorological parameter	*NW-SE air*	*SW air*
NO (pptv)	142	233
NO_2 (pptv)	1854	2766
HONO (pptv)	52	97
CO (ppbv)	113	106
O_3 (ppbv)	39	31
HCHO (pptv)	925	1127
Isoprene (pptv)	27	34
MVK+MACR (pptv)	40	88
$PM_{2.5}$ ($\mu g/m^3$)	3.8	4.4
Temp (°C)	15.7	17.4
RH (%)	82	72
$J(O^1D)$ (s^{-1})[a]	1.7×10^{-5}	1.4×10^{-5}

[a] Reported as the maxima in Figure S3.

Table S2. Fit parameters obtained from power law fits ($y = y0 + Ax^{pow}$) to the OH vs $J(O^1D)$ data shown in Figure S6, split according to wind direction (NW–SE = <165° and >285°; SW = 180°–270°).

	NW-SE		***SW***	
	Observed	*MCM-base*	*Observed*	*MCM-base*
*y*0	1.2×10^5	1.4×10^4	1.8×10^5	1.0×10^5
A	7.2×10^{11}	3.7×10^9	1.1×10^{10}	5.2×10^{10}
pow	0.86	0.61	0.67	0.80

Table S3. Fit parameters obtained from linear fits (y = mx + c, with number of points, N, and Pearson correlation coefficient, R) to the RO_2 vs HO_2 data shown in Figure 4 of the main paper, split according to wind direction (NW–SE = <165° and >285°; SW = 180°–270°).

	NW-SE		***SW***	
	Observed	*MCM-base* [a]	*Observed*	*MCM-base* [a]
m	1.3	0.67	1.8	0.63
c	1.6×10^8	9.6×10^6	1.20×10^8	-3.50×10^6
N	373	113	451	122
R	0.63	0.96	0.81	0.97

[a] Nighttime data not included.

Supplementary Figures S1 – S5.

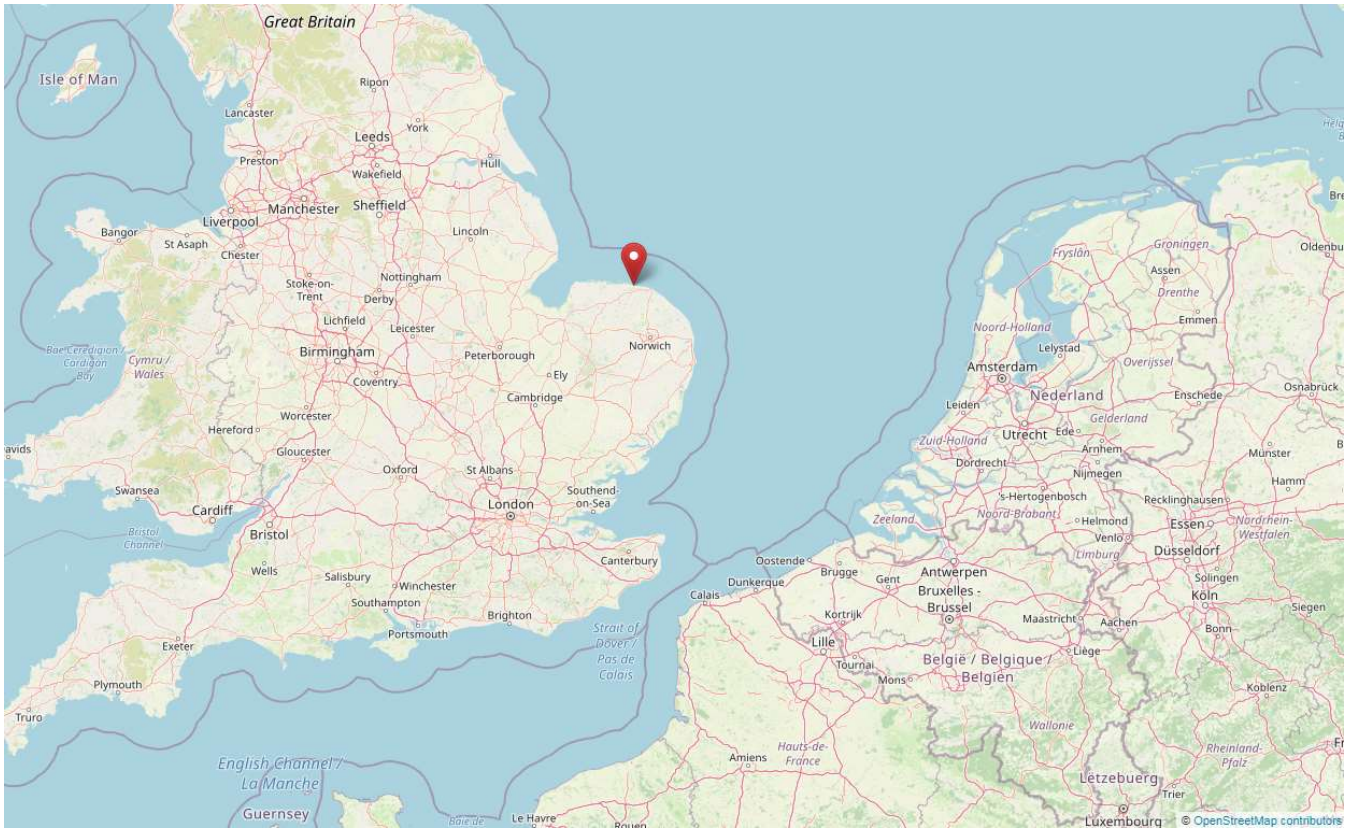

Figure S1. Location (red pin) of the Weybourne Atmospheric Observatory (WAO) on the North Norfolk coast (52°57'02" N, 1°07'19"E, 16 m above sea level). © OpenStreetMap contributors 2022. Distributed under the Open Data Commons Open Database License (ODbL) v1.0.

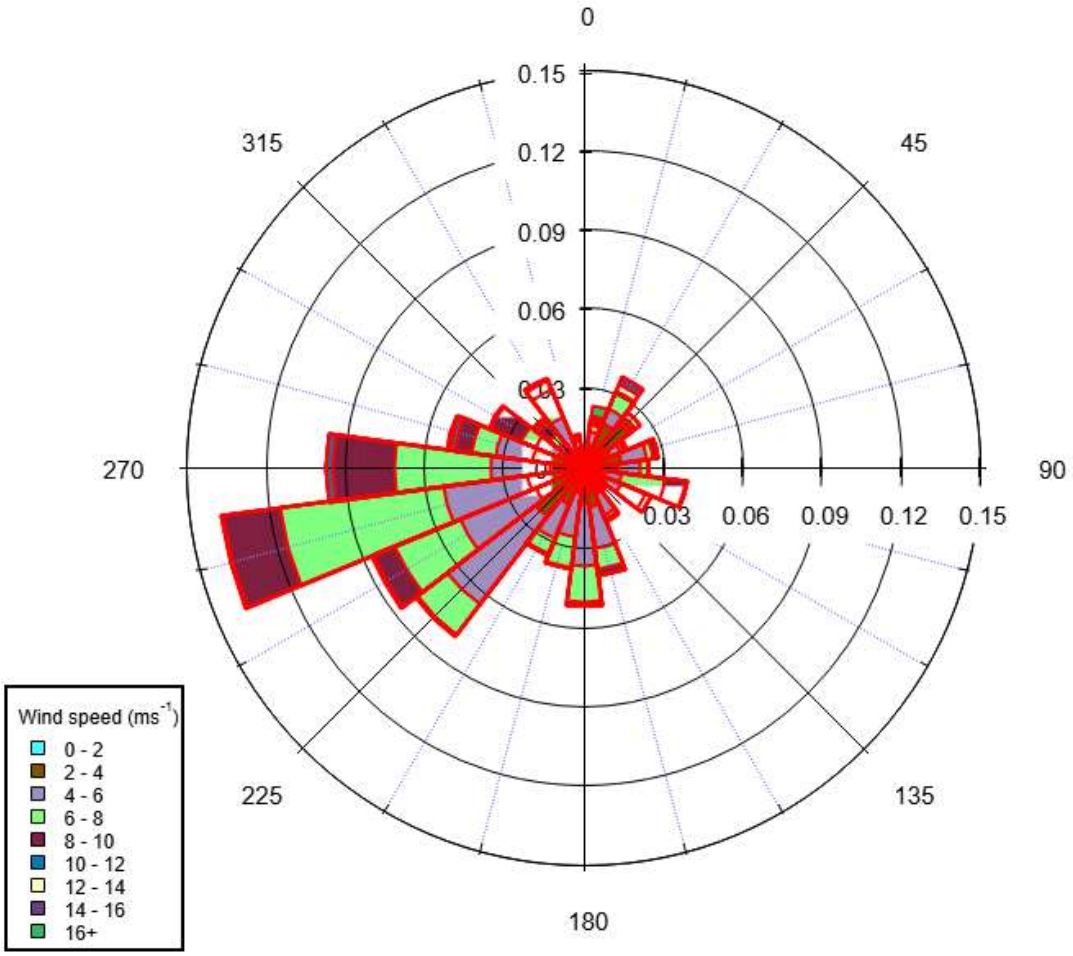

Figure S2. Wind rose plot for the entire campaign. Air originated from the SW sector (180°–270°) for approximately 50% of the time.

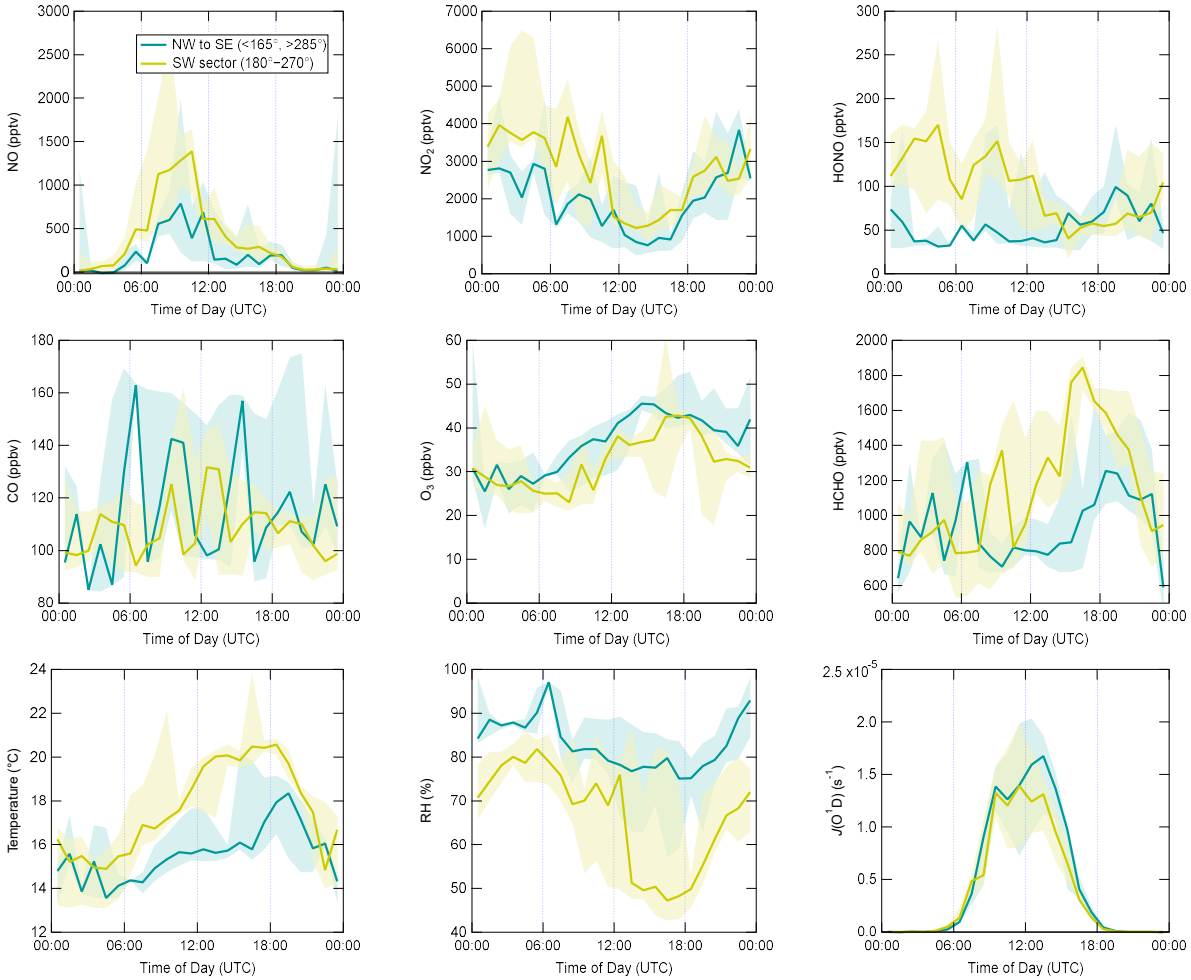

Figure S3. Diel profiles of trace gases and meteorological parameters, split according to wind direction (NW–SE = <165° and >285°; SW = 180°–270°). Data were only included if radical measurements were also available. Shaded areas correspond to 25th and 75th percentiles of the data in each time bin.

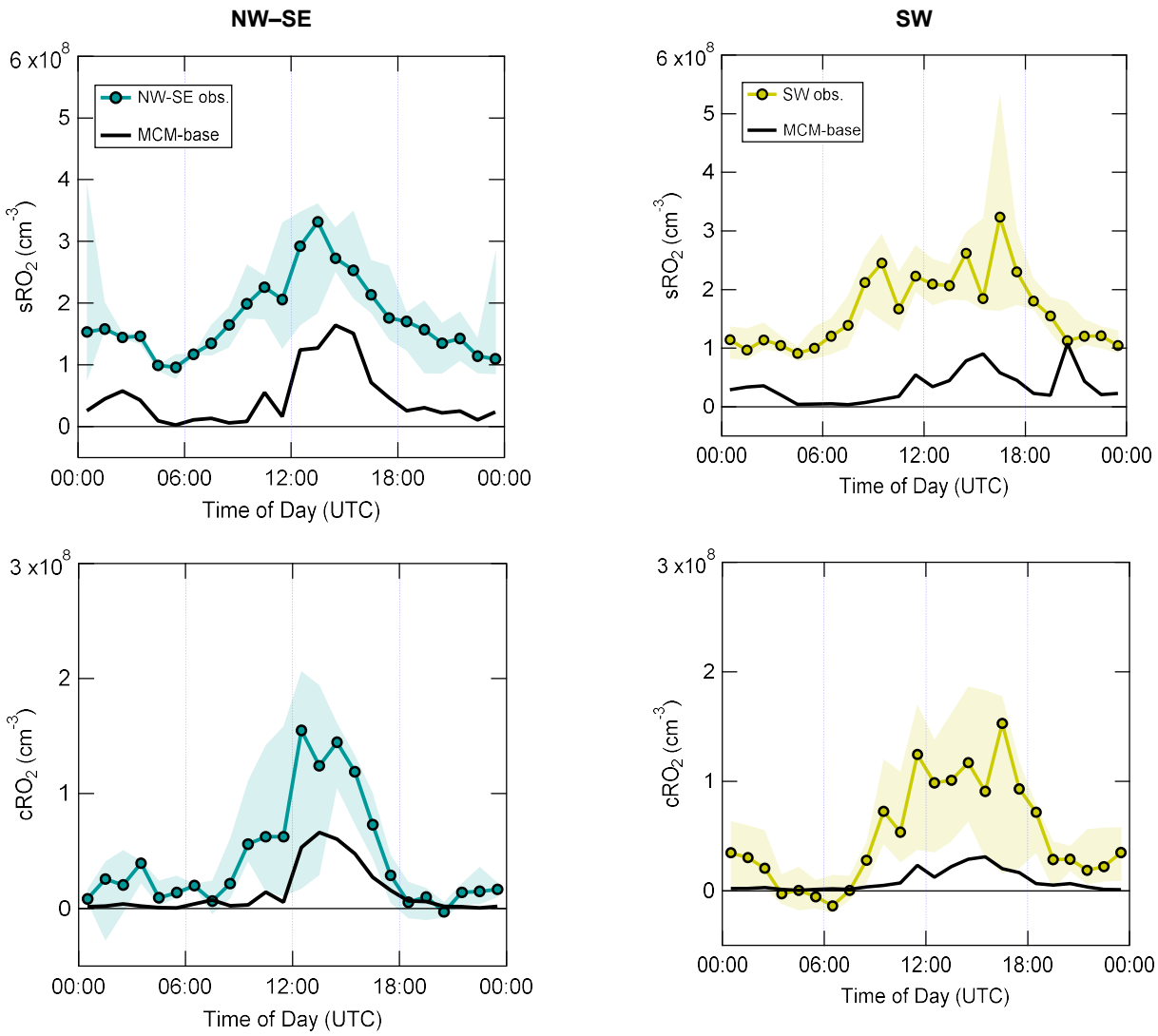

Figure S4. Hourly median diel profiles of "simple" (sRO_2) and "complex" RO_2 (cRO_2), defined in text, and comparison to MCM-base model predictions, split according to wind direction (left NW–SE, right SW).

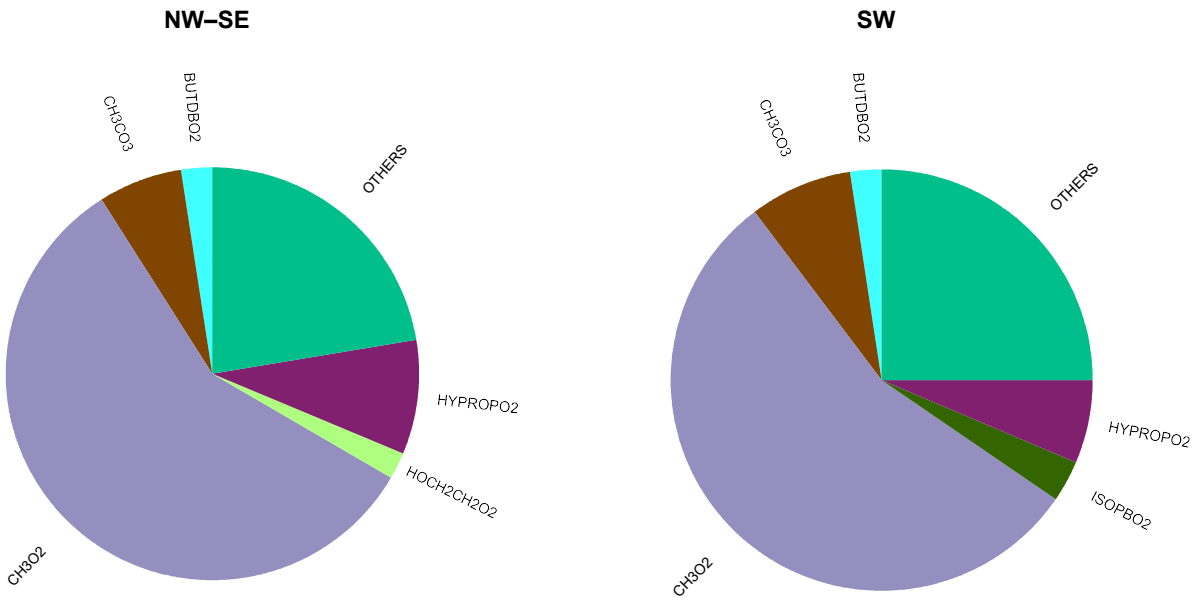

Figure S5. Daytime median RO_2 contributions predicted by the MCM-base model, split according to wind direction (left: NW–SE, right: SW). For clarity, only the top five RO_2 species are shown, otherwise the RO_2's are lumped together as "others". MCM nomenclature used, definitions are HYPROPO2 ($CH_2(OH)CH(CH_3)O_2$, formed from OH addition to propene) with a contribution of ~9%, followed by acetylperoxy (CH_3CO_3, ~7%), BUTDBO2 ($CH_2(OH)CH(O_2)CH{=}CH_2$, formed from OH addition to 1,3-butadiene, ~2%), and HOCH2CH2O2 ($CH_2(OH)CH_2O_2$, formed from OH addition to ethene, ~2%). Other RO_2 radicals contribute ~22% in total. In SW air, the contributions are fairly similar: HYPROPO2 ~6%, acetylperoxy ~8%, BUTDBO2 ~2%, and HOCH2CH2O2 ~2%. Other RO_2 radicals are slightly more important than in NW–SE air, with a total contribution of ~25%. Isoprene-derived peroxy radicals (with the most important being ISOPBO2 and ISOPDO2) contribute only ~2% and ~5% in NW–SE and SW air, respectively.

Supplementary Text S1-S3, Table S4 and Figures S6 – S11

S1. Comparison to previous coastal field campaigns

Table S4 summarises previous measurements of OH, HO_2, HO_2+RO_2 and OH reactivity at the WAO site, and also at other selected locations in the MBL. A more detailed summary up until 2012 can be found in Stone et al., 2012. For other ground and ship-based campaigns in the MBL, measured noontime OH concentrations were mostly in the range ~4–6 × 10^6 molecule cm^{-3}, and generally the observations have been found to agree with model predictions to within ~30% on average during the daytime in the MBL (Sommariva et al., 2004; Sommariva et al., 2006; Whalley et al., 2010; Beygi et al., 2011; Van Stratum et al., 2012). During the NASA airborne Atmospheric Tomography study (ATom), OH concentrations in the MBL were on the order of ~1–4 × 10^6 molecule cm^{-3} and a model was able to reproduce them to generally within 40% (Brune et al., 2020). In NAMBLEX HO_2 levels were overpredicted by up to a factor of 2 (Sommariva et al., 2006). These results are almost identical to the findings of ICOZA despite the substantial differences in chemical conditions (e.g., the much lower anthropogenic influence and the role of halogen species during NAMBLEX). For other campaigns, HO_2 concentrations were generally above ~2 × 10^8 molecule cm^{-3} (Sommariva et al., 2004; Whalley et al., 2010; Beygi et al., 2011), higher than the range observed during ICOZA (~0.5–2 × 10^8 molecule cm^{-3}), and the observations have mostly been overpredicted. During ATom, HO_2 concentrations in the MBL were on the order of ~1–5 × 10^8 molecule cm^{-3} and were well captured by a model (agreement within 40%) (Brune et al., 2020). The mean missing OH reactivity in terms of the difference between measured OH reactivity and that calculated using trace gases only was 1.9 s^{-1} (39%) during TORCH 2 (cf. 2.1 s^{-1}, 42% for ICOZA). A box model using MCMv3.1 chemistry (Bloss et al., 2005) was used to simulate OH reactivity, reducing the missing reactivity to 1.4 s^{-1} or 29% (cf. 1.7 s^{-1}, 36% for ICOZA). Lee et al. (2009) speculated that the missing reactivity may be due to a potentially large number of unmeasured, high molecular weight aromatic compounds, but that this could also be due to missing OVOCs, as we have suggested based on the data in Figure S9. To date, only a handful of studies have measured OH reactivity at coastal locations (examples in Table S4) but there have been airborne campaigns conducted in the marine boundary layer. An airborne OH reactivity instrument was deployed during flights over the Pacific Ocean for the Intercontinental Chemical Transport Experiment-B (INTEX-B) campaign (Mao et al., 2009). In the boundary layer (i.e., < 2 km altitude), measured OH reactivity was ~4 s^{-1} on average, while that calculated from measured reactants was only ~1.5–2 s^{-1} (i.e., ~50–60% missing), similar to ICOZA. During the NASA Atmospheric Tomography (ATom) campaign involving flights over the Atlantic and Pacific Oceans, measured OH reactivity at < 2 km was on the order of ~2 s^{-1}, with missing reactivity on the order of ~0.5–1 s^{-1} (~25–50% missing) (Thames et al., 2020). The authors suggested that, based on correlations of missing OH reactivity with HCHO, DMS, butanal, and sea surface temperature, there were unmeasured/unknown VOCs/OVOCs associated with oceanic emissions, in agreement with our findings.

Table S4. Previous measurements of OH, HO_2, sum of HO_2+RO_2 and OH reactivity at WAO and other selected locations in the MBL.

Campaign, location and date	Concentration of NO	OH peak concentration / molecule cm^{-3}	HO_2 peak concentration / molecule cm^{-3}	HO_2+RO_2 peak concentration/ molecule cm^{-3}	OH reactivity / s^{-1}	References
ICOZA, WAO[a], June/July 2015	mean 0.38 ppbv range ~0–7.5 ppbv	~4×10^6 (noon)	1×10^8 (~2 pm)	~4-6 $\times 10^8$ (noon) 2×10^8 (night)	5.0 s^{-1} (mean) 17.6 s^{-1} (max)	This work
TORCH[b] 2, WAO, May 2004	mean 0.62 ppbv range ~0–50 ppbv	~4×10^6 (noon)	~8×10^7		4.9 s^{-1} (mean) 9.7 s^{-1} (peak)	Smith, 2007; Lee et al., 2009
WAO, 1995		~4–7 $\times 10^6$ (measured using DOAS)	~4–7 $\times 10^6$ (measured using DOAS)			Forberich et al., 1999; Grenfell et al., 1999
NAMBLEX[c], Mace Head, 2002	Range 7-70 pptv	~4×10^6	0.9–2.1 $\times 10^8$			Heard et al., 2006
DOMINO[d], SW Spain, Nov–Dec 2008			1.5×10^8	~2–12 $\times 10^8$ (day) ~20×10^8 (nighttime spikes) (PERCA)		Van Stratum et al., 2012; Andres-Hernandez et al., 2013; Sinha et al., 2012
Various at WAO, including INSPECTRO [f], Sept 2002				~2–5 $\times 10^8$ (day) ~5–7 $\times 10^7$ (night) (PERCA[e])		Penkett et al., 1999; Fleming et al., 2006; Green et al., 2006
EASE 97, Mace Heard, Apr-May 1997	Range 75 –400 pptv	2-6 $\times 10^6$ (noon)	0.5– 3.5 $\times 10^8$ (noon)	~1×10^8 (night) (PERCA)		Salisbury et al., 2001; Creasey et al., 2002; Carslaw et al., 2002
TexAQS, Ship-based off coast near Houston 2006 [g]				~30×10^8 (nighttime, polluted) ~2–10 $\times 10^8$ (nighttime, clean) (PERCA)		Sommariva et al., 2011
Corsica, Summer 2013					~5 s^{-1} (mean), ~17 s^{-1} (max) with CRM[h]	Zannoni et al., 2017

[a] Weybourne Atmospheric Observatory
[b] Tropospheric ORganic photoCHemistry experiment
[c] North Atlantic Marine Boundary Layer Experiment
[d] Diel Oxidants Mechanisms In relation to Nitrogen Oxides
[e] peroxy radical chemical amplification
[f] Influence of clouds on the spectral actinic flux in the lower troposphere
[g] Texas Air Quality Study
[h] Comparative reactivity method

S2. Further discussion of the results for the different MCM model runs

The carbonyls HCHO and MVK+MACR were not constrained in the MCM-base model because of several gaps in the time series of these measurements. The MCM-base model performance in simulating these carbonyls was assessed, where it was found that there was reasonable agreement for MVK+MACR on a diel average basis, but that HCHO concentrations were significantly overpredicted in the afternoon (data not shown). The differences in the calculated concentrations of these OVOC compounds is the cause of the differences between the MCM-base and MCM-carb simulations of radical species (Figure 3). Similarly, HO_2 concentrations were generally overpredicted by both the MCM-base and MCM-carb models, and therefore constraining to HO_2 (MCM-hox model) has impacts on the model OH and RO_2 concentrations (Figure 3). Since the MCM-base model also underpredicted OH reactivity, there are additional differences between the PSS calculation of OH and the MCM model predictions.

For OH, differences between the MCM-base and MCM-carb runs are relatively minor and both positive and negative (Figure 3). There are two competing effects here: HCHO is a minor OH sink (~6% and thus an overprediction of HCHO would lead to lower OH in MCM-base relative to MCM-carb. In contrast, the base model overprediction of HCHO leads to a greater HO_2 source strength that would drive higher OH levels in MCM-base relative to MCM-carb. Similarly, HO_2 was overpredicted in MCM-base and MCM-carb such that constraining the model to HO_2 (MCM-hox) resulted in lower model OH levels. Finally, due to the MCM model underprediction of OH reactivity, PSS calculated OH levels were lower than the MCM model concentrations. At low NO (Figure S7), the better agreement found for the OH/MCM-base case compared to the OH/PSS case is driven by the MCM overprediction of HO_2, i.e., the agreement for OH does not necessarily mean the OH chemistry is well understood at low NO. Peak afternoon RO_2 concentrations were similar for the MCM-base and MCM-carb simulations (Figure 3). However, the reduced OH in MCM-hox results in reduced afternoon RO_2 levels.

S3. Observed and modelled OH versus $J(O^1D)$

Since OH is formed photochemically with ozone photolysis as a major source (Reaction (R1); OH levels are known to display a strong dependence on $J(O^1D)$. Strong correlations between OH and $J(O^1D)$ have been found for many field campaigns in a range of different environments (Ehhalt, 1999; Brauers et al., 2001; Creasey et al., 2003; Rohrer and Berresheim, 2006; Smith et al., 2006; Bloss et al., 2007; Emmerson et al., 2007; Smith, 2007; Furneaux, 2009; Lu et al., 2012; Vaughan et al., 2012; Lu et al., 2013; Tan et al., 2017; Tan et al., 2018). In the present work, observed and modelled OH concentrations are plotted against $J(O^1D)$ for NW–SE and SW air in Figure S6. Here, the data were split into 12 bins with the same number of points, to spread data evenly across the full range of $J(O^1D)$. Power law fits ($y = y0 + Ax^{pow}$) were applied to the datasets for comparison of fit parameters to previous work. The fit parameters may be interpreted as follows: (1) the intercept (y0) is a measure of OH production which does not require the presence of light, for example alkene ozonolysis (but which can also occur during the day); (2) the scaling factor (A) reflects the dependence of OH on other species such as NO_x and VOCs; (3) the power term

(pow) represents the combined effects of photolytic processes (Rohrer and Berresheim, 2006). The fit parameters obtained are summarised in Table S2. In NW–SE air, measured OH concentrations exhibit an almost linear dependence on $J(O^1D)$, with a power term of 0.86. The fit to modelled OH exhibits more curvature, close to a square root dependence, and an intercept smaller than that for the measurements by a factor of 10. In SW air, the measured dependence is less linear (power term = 0.67) but the intercept is similar to that for NW–SE air. In contrast to NW–SE air, the measurement and model curves are similar such that either can describe the data reasonably well. Overall, the power terms are amongst the lower values of previous reports, which ranged from 0.61–1.3 (Stone et al. (2012) and references therein). These power terms are most similar to those found for other coastal campaigns such as at Mace Head, Ireland (0.84; (Smith et al., 2006)) and Finokalia, Crete (0.68; (Berresheim et al., 2003)).

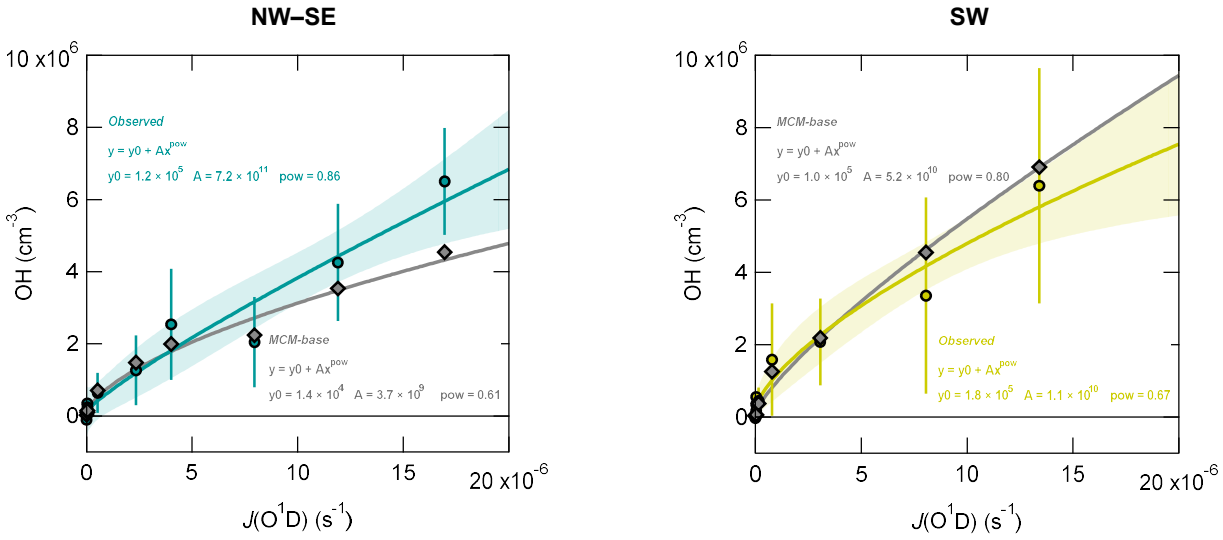

Figure S6. Observed and modelled OH binned against $J(O^1D)$ using 12 bins with approximately the same number of points, split according to wind direction (left NW–SE, right SW). Data are shown as means, where error bars on measurement points correspond to one standard deviation (SD, not shown for model data for clarity). Solid lines are power law fits to OH vs $J(O^1D)$, and shaded areas give 95% confidence intervals of the fits to observed data (not shown for model data for clarity).

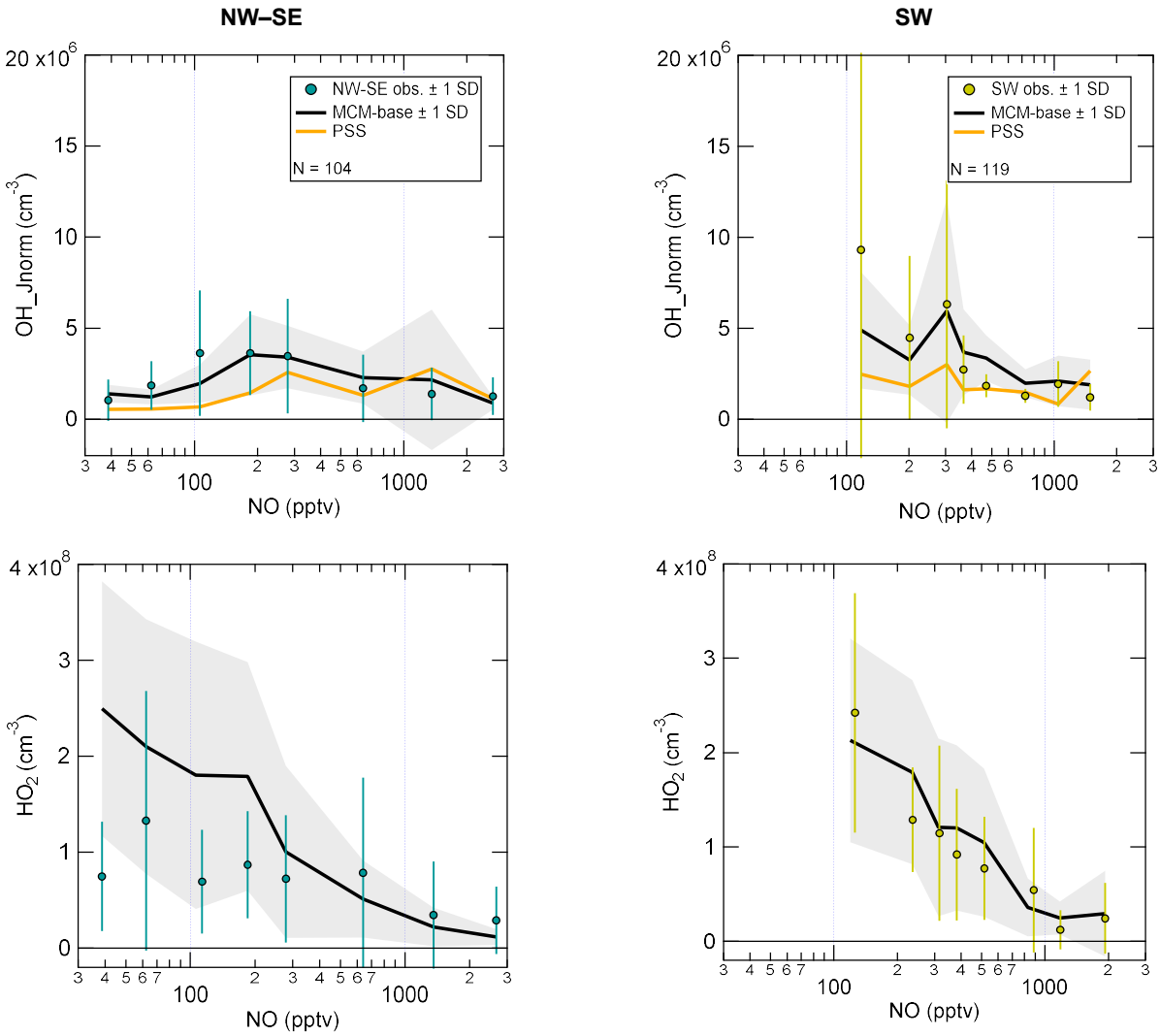

Figure S7. Caption on next page.

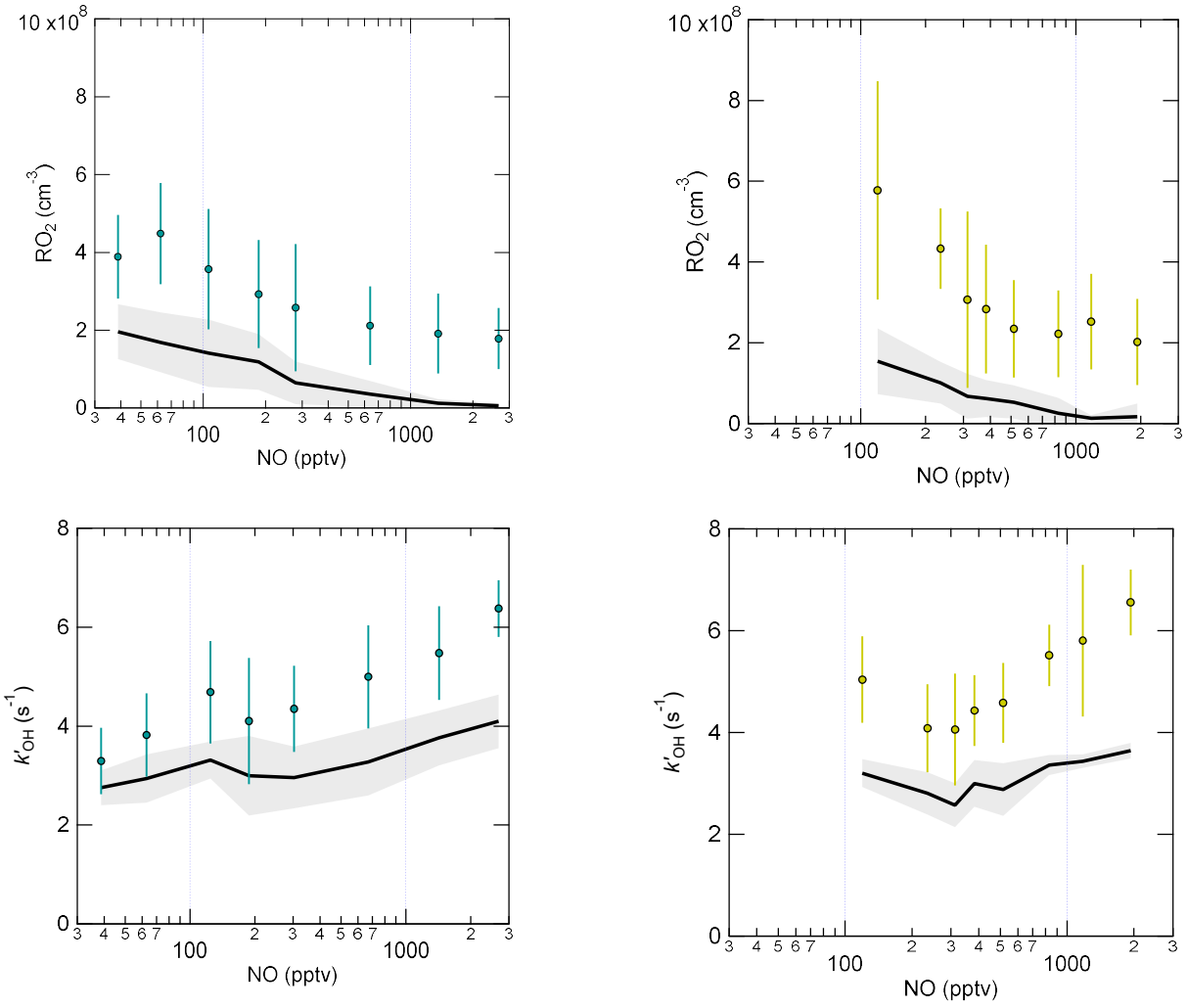

Figure S7 (cont'd). Dependence of observed and modelled OH (normalised to average $J(O^1D)$), HO_2, total RO_2, and OH reactivity on NO mixing ratios. Only daytime data were included, using the filter $J(O^1D) > 5 \times 10^{-7}$ s^{-1}. Data are shown as means ± 1 SD, and split according to wind direction (left NW–SE, right SW). Data were separated into 8 NO bins with approximately the same number of points.

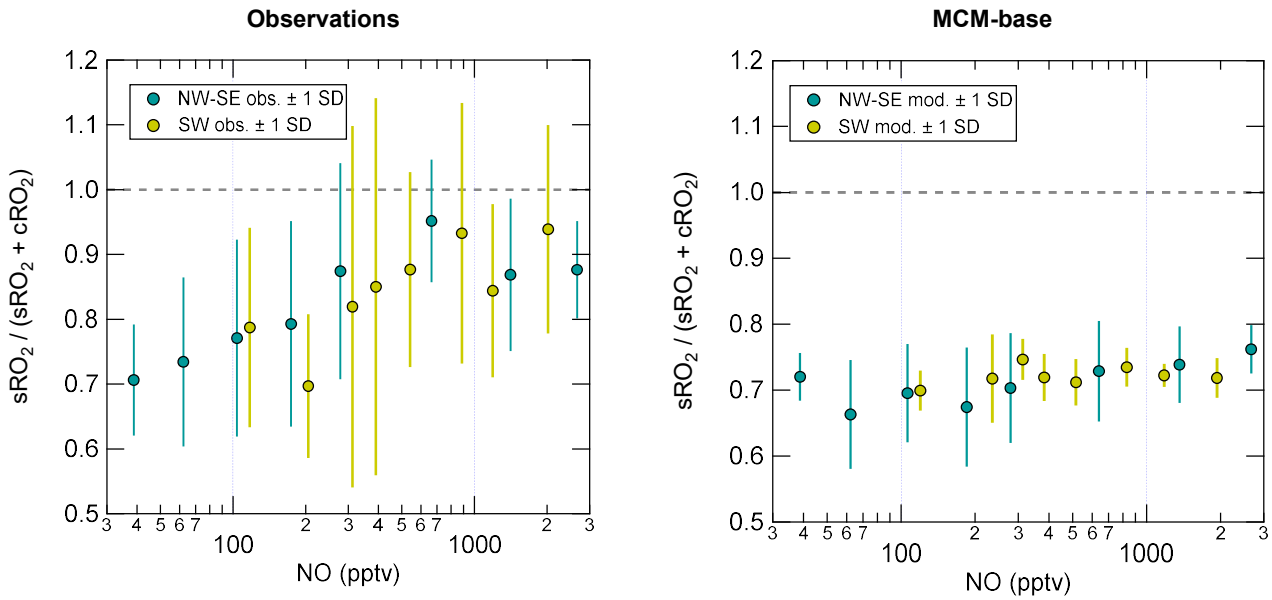

Figure S8. Contribution of sRO_2 to total RO_2 (= sRO_2 + cRO_2) as a function of NO (measurements left, model results right). Data are shown as means ± 1 SD. Data were separated into 8 NO bins with approximately the same number of points.

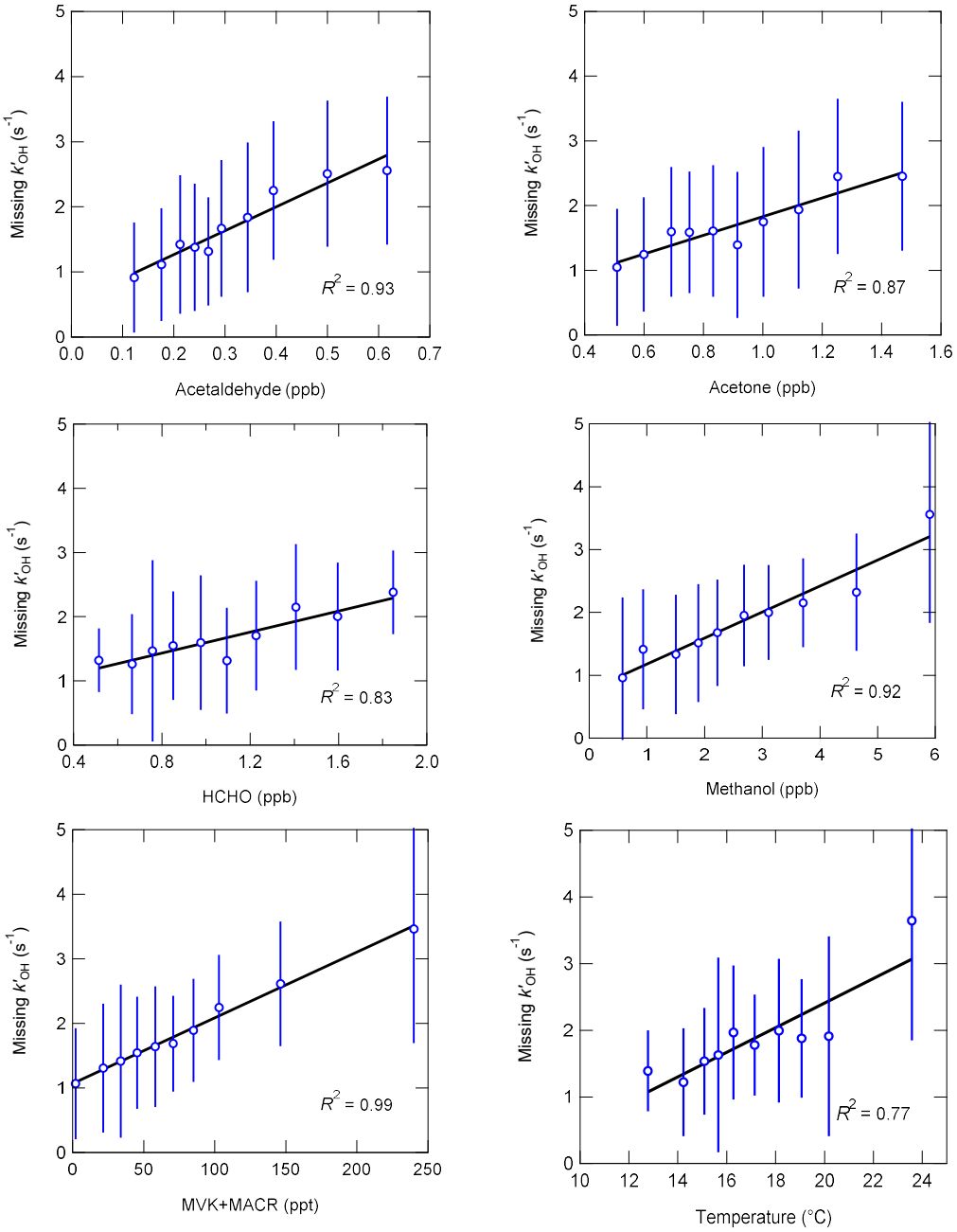

Figure S9. Dependence of missing OH reactivity (defined as the difference between measured and modelled OH reactivity) on acetaldehyde, acetone, HCHO, methanol, MVK+MACR, and temperature. Data are shown as means ± 1 SD. In each plot, data were separated into 10 *x*-bins with approximately the same number of points.

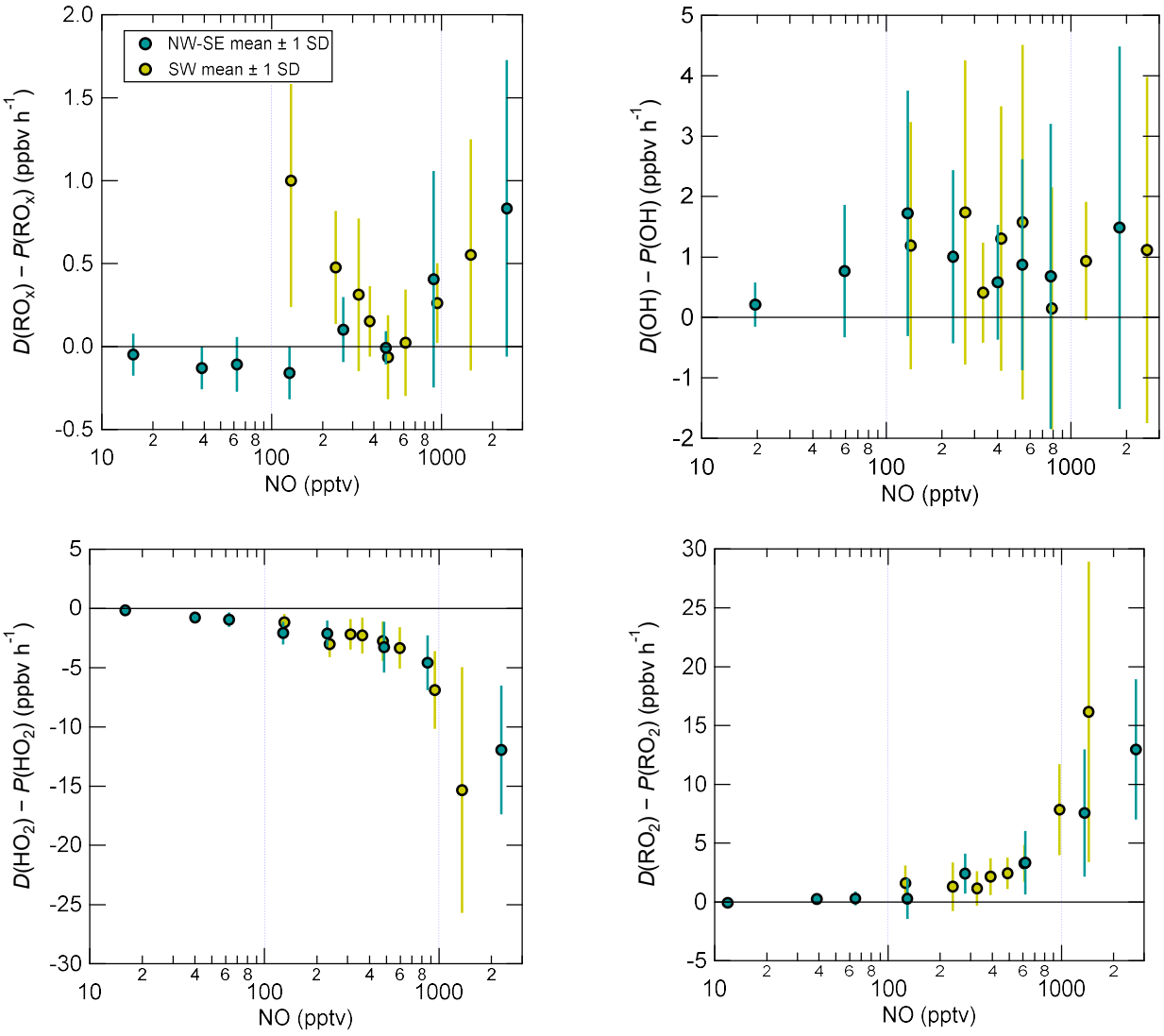

Figure S10. Destruction minus production (i.e., budget imbalance) as a function of NO for RO_x (top left), OH (top right), HO_2 (bottom left), and RO_2 (bottom right) in NW–SE and SW air. Daytime points only, with daytime defined as $J(O^1D) > 5 \times 10^{-7}$ s^{-1}. Data were separated into 8 bins with an approximately equal number of points. Data points are shown as means ± one standard deviation (SD). Note *x*-log scale.

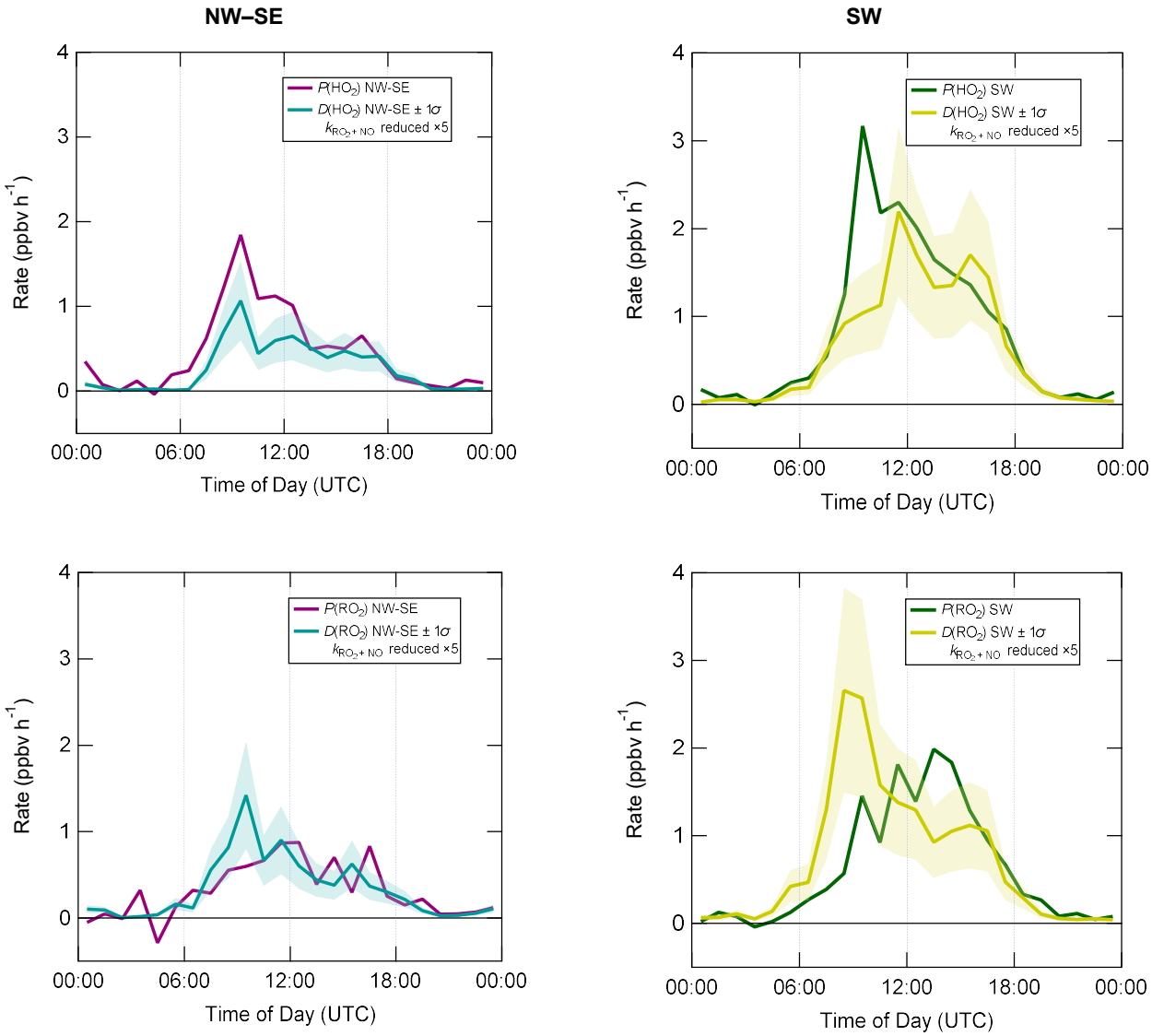

Figure S11. HO_2 (top) and RO_2 (bottom) budgets after artificially reducing the RO_2 + NO rate coefficient by a factor of 5.

Supplementary text S4-S5, Figures S12-S15

S4. Inclusion of heterogeneous uptake on the HO_2 budget calculations

Up to now, the heterogeneous uptake of HO_2 has not been considered in the HO_2 budget calculations. The heterogeneous loss of HO_2 was parametrised using the following first-order loss rate (Ravishankara, 1997):

$$k'_{loss} = \omega A \gamma / 4 , \quad \text{(E1)}$$

where ω is the mean molecular speed of HO_2 (43725 cm s^{-1} at 298 K), A is the aerosol surface area measured by the aerodynamic particle sizer (APS), and γ is the aerosol uptake coefficient. Using γ = 0.1, a value consistent with previous laboratory experiments (Mozurkewich et al., 1987; George et al., 2013; Lakey, 2014; Lakey et al., 2015; Lakey et al., 2016; Moon, 2018) and the same value used in the MCM model, the impact on the HO_2 budget is negligible, as shown in Figure S12. Even increasing γ to unity has virtually no effect on $D(HO_2)$, due to the low particulate matter loading observed during ICOZA ($A \sim 0.6–4.2 \times 10^{-7}$ cm^2 cm^{-3}).

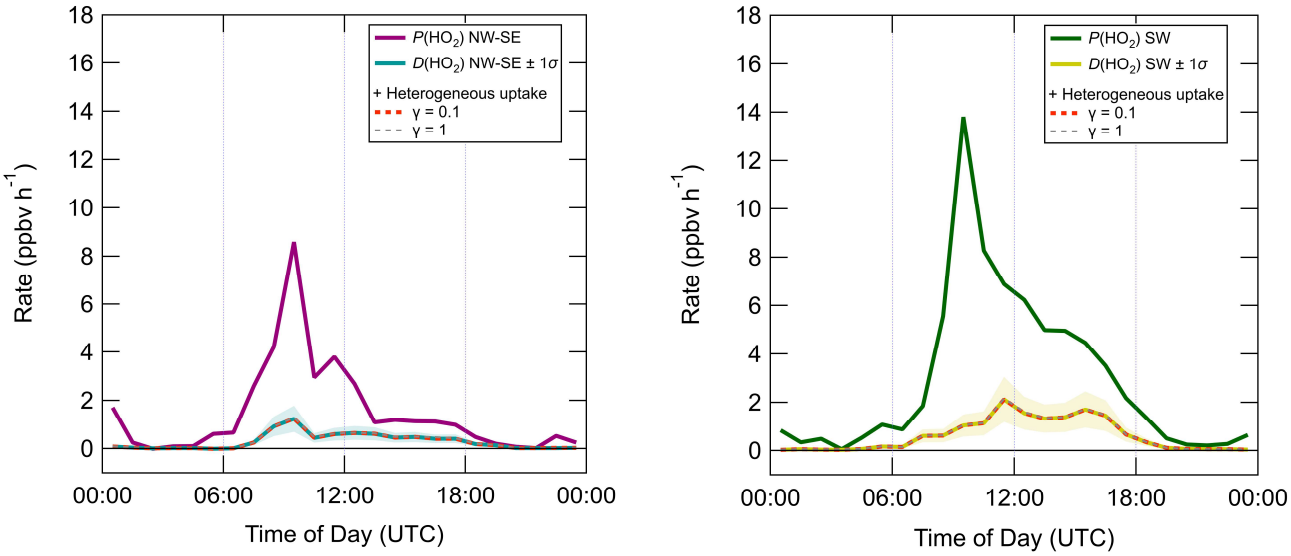

Figure S12. HO_2 budget after inclusion of heterogeneous uptake using different γ_{HO2}.

S5. Inclusion of chlorine atom initiated oxidation chemistry

A missing primary RO_2 source has been invoked previously to help explain model underpredictions of RO_2 (Tan et al., 2017) in which it was hypothesised that reactions of chlorine atoms (e.g., from the photolysis of Cl_2 or $ClNO_2$ (Osthoff et al., 2008)) with VOCs during the morning were the source of the missing RO_2, although the contribution was not sufficient to

explain the magnitude of the RO_2 underprediction (inclusion of Cl chemistry accounted for only ~10–20% of the missing RO_2). Cl_2 and $ClNO_2$ were both measured during ICOZA (Sommariva et al., 2018), such that their impact on the RO_2 budget can be assessed. Assuming that all photolysed Cl atoms react with VOCs, rather than with inorganic species, i.e., $P(\text{Cl-RO}_2) \approx P(\text{Cl}) = 2J(\text{Cl}_2)[\text{Cl}_2] + J(\text{ClNO}_2)[\text{ClNO}_2]$, an upper limit of the impact of chlorine chemistry can be derived. Figure S13 shows that even this upper limit contribution has negligible impacts on the RO_2 budget, ruling out chlorine chemistry as the source of the RO_2 budget discrepancy. In NW–SE air, the upper limit contribution from chlorine chemistry ($P(\text{Cl-RO}_2)$) peaked in the morning at ~0.08 ppbv h^{-1}, but peaked in the afternoon in SW air at ~0.12 ppbv h^{-1}, in comparison to $P(RO_2)$ and $D(RO_2)$ values of up to ~2 and ~14 ppbv h^{-1}, respectively These results are consistent with a previous report of the small impact of chlorine oxidation at the WAO (Bannan et al., 2017).

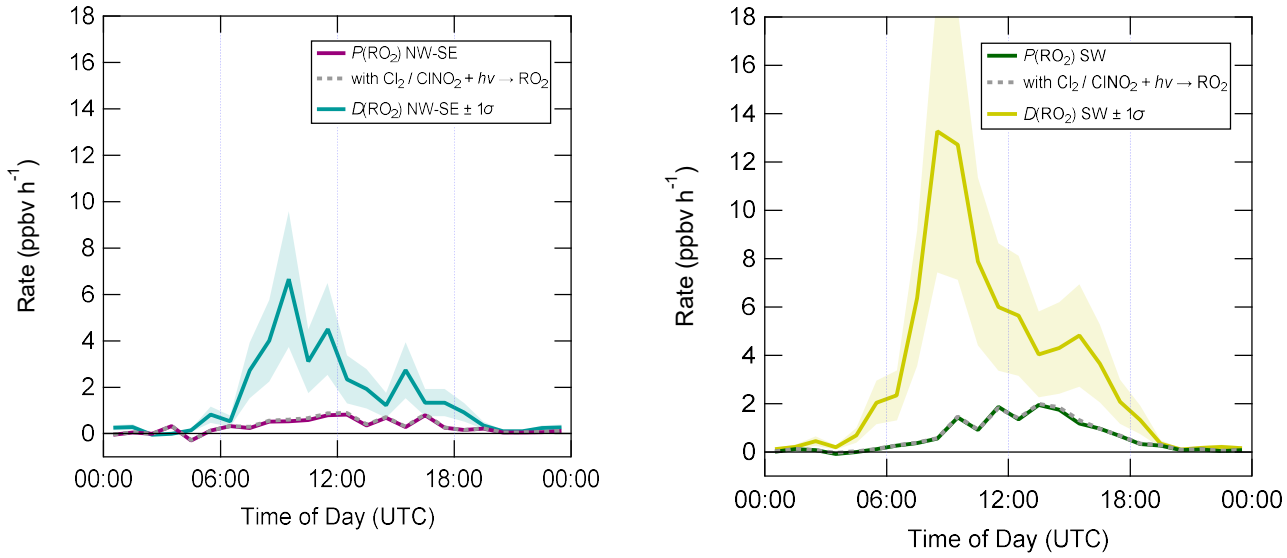

Figure S13. RO_2 budget after inclusion of chlorine chemistry. All photolysed Cl atoms are assumed to react with VOCs to yield RO_2, i.e., $Cl_2/ClNO_2 \rightarrow n\text{Cl} \rightarrow n\text{RO}_2$, where $n = 2$ for Cl_2 and $n = 1$ for $ClNO_2$. This assumption therefore yields an upper limit for the impact of chlorine chemistry.

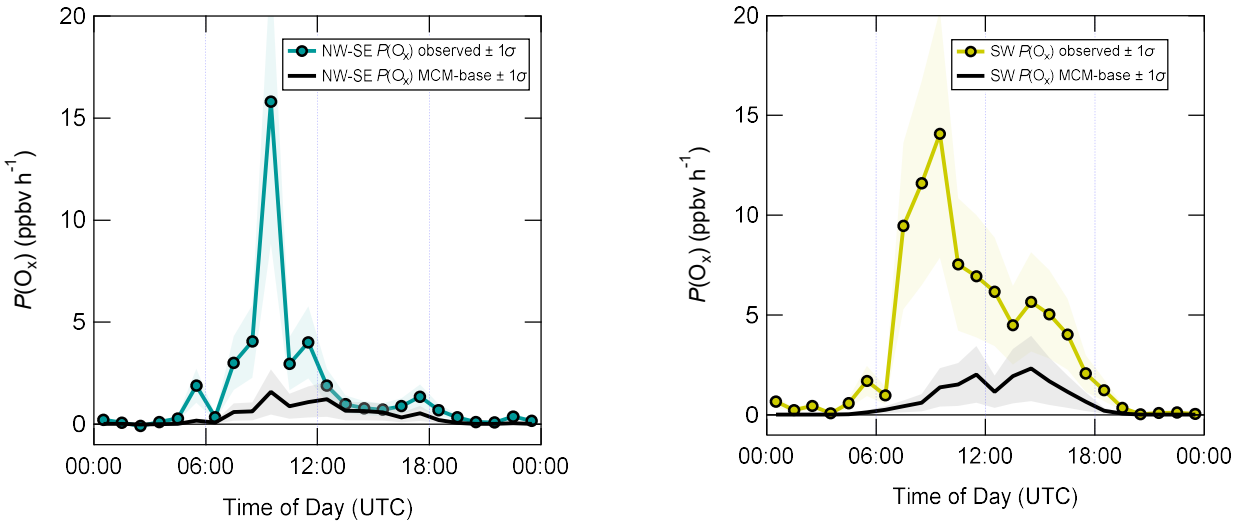

Figure S14. Median diel profiles of $P(O_x)$, defined in equations (E12–E14), as calculated from measured and MCM-base model HO_2 and RO_2, split according to wind direction. Shaded areas correspond to estimated 1σ uncertainties of 40% and 70% for measured and model $P(O_x)$, respectively.

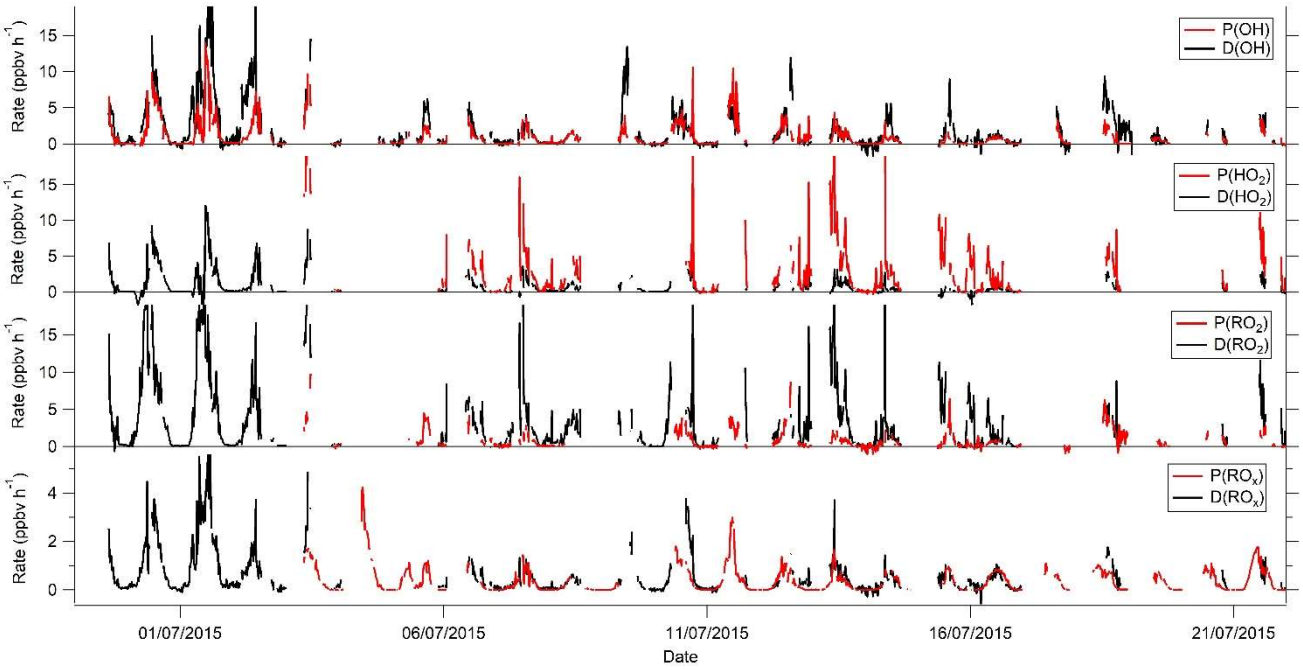

Figure S15. A time series of the experimentally determined radical budgets for the ICOZA campaign, which demonstrates the variability of the total rate of production (P) and the total rate of destruction (D) for OH, HO_2, RO_2 and RO_x (=sum of OH, HO_2 and RO_2).

Supplementary Information References.

Andres-Hernandez, M. D., Kartal, D., Crowley, J. N., Sinha, V., Regelin, E., Martinez-Harder, M., Nenakhov, V., Williams, J., Harder, H., Bozem, H., Song, W., Thieser, J., Tang, M. J., Beigi, Z. H., and Burrows, J. P.: Diel peroxy radicals in a semi-industrial coastal area: nighttime formation of free radicals, Atmos Chem Phys, 13, 5731-5749, 10.5194/acp-13-5731-2013, 2013.

Bannan, T. J., Bacak, A., Le Breton, M., Flynn, M., Ouyang, B., McLeod, M., Jones, R., Malkin, T. L., Whalley, L. K., Heard, D. E., Bandy, B., Khan, M. A. H., Shallcross, D. E., and Percival, C. J.: Ground and Airborne U.K. Measurements of Nitryl Chloride: An Investigation of the Role of Cl Atom Oxidation at Weybourne Atmospheric Observatory, Journal of Geophysical Research: Atmospheres, 122, 11,154-111,165, 10.1002/2017jd026624, 2017.

Berresheim, H., Plass-Dülmer, C., Elste, T., Mihalopoulos, N., and Rohrer, F.: OH in the coastal boundary layer of Crete during MINOS: Measurements and relationship with ozone photolysis, Atmos. Chem. Phys., 3, 639-649, 10.5194/acp-3-639-2003, 2003.

Beygi, Z. H., Fischer, H., Harder, H. D., Martinez, M., Sander, R., Williams, J., Brookes, D. M., Monks, P. S., and Lelieveld, J.: Oxidation photochemistry in the Southern Atlantic boundary layer: unexpected deviations of photochemical steady state, Atmos Chem Phys, 11, 8497-8513, 10.5194/acp-11-8497-2011, 2011.

Bloss, C., Wagner, V., Jenkin, M. E., Volkamer, R., Bloss, W. J., Lee, J. D., Heard, D. E., Wirtz, K., Martin-Reviejo, M., Rea, G., Wenger, J. C., and Pilling, M. J.: Development of a detailed chemical mechanism (MCMv3.1) for the atmospheric oxidation of aromatic hydrocarbons, Atmos Chem Phys, 5, 641-664, DOI 10.5194/acp-5-641-2005, 2005.

Bloss, W. J., Lee, J. D., Heard, D. E., Salmon, R. A., Bauguitte, S. J. B., Roscoe, H. K., and Jones, A. E.: Observations of OH and HO_2 radicals in coastal Antarctica, Atmos Chem Phys, 7, 4171-4185, DOI 10.5194/acp-7-4171-2007, 2007.

Brauers, T., Hausmann, M., Bister, A., Kraus, A., and Dorn, H. P.: OH radicals in the boundary layer of the Atlantic Ocean 1. Measurements by long-path laser absorption spectroscopy, J Geophys Res-Atmos, 106, 7399-7414, Doi 10.1029/2000jd900679, 2001.

Brune, W. H., Miller, D. O., Thames, A. B., Allen, H. M., Apel, E. C., Blake, D. R., Bui, T. P., Commane, R., Crounse, J. D., Daube, B. C., Diskin, G. S., DiGangi, J. P., Elkins, J. W., Hall, S. R., Hanisco, T. F., Hannun, R. A., Hintsa, E. J., Hornbrook, R. S., Kim, M. J., McKain, K., Moore, F. L., Neuman, J. A., Nicely, J. M., Peischl, J., Ryerson, T. B., St. Clair, J. M., Sweeney, C., Teng, A. P., Thompson, C., Ullmann, K., Veres, P. R., Wennberg, P. O., and Wolfe, G. M.: Exploring Oxidation in the Remote Free Troposphere: Insights From Atmospheric Tomography (ATom), J Geophys Res-Atmos, 125, e2019JD031685, https://doi.org/10.1029/2019JD031685, 2020.

Carslaw, N., Creasey, D.J., Heard, D. E., Jacobs, P.J., Lee, J. D., Lewis, A. C., McQuaid, J. B., Pilling, M. J., Bauguitte, S., Penkett, S.A., Monks, P.S. and Salisbury, G., Eastern Atlantic Spring Experiment 1997 (EASE97). 2. Comparisons of model concentrations of OH, HO_2 and RO_2 with measurements, J. Geophys. Res., 107 (D14), 10.1029/2001JD001568, 2002.

Creasey, D. J., Halford-Maw, P. A., Heard, D. E., Pilling, M. J., and Whitaker, B. J.: Implementation and initial deployment of a field instrument for measurement of OH and HO_2 in the troposphere by laser-induced fluorescence, J Chem Soc Faraday T, 93, 2907-2913, DOI 10.1039/a701469d, 1997.

Creasey, D. J., Heard, D. E., Lee, J. D.: Eastern Atlantic Spring Experiment 1997 (EASE97): 1. Measurements of OH and HO_2 concentrations at Mace Head, Ireland, J. Geophys. Res-Atmos, 107 (D10), 4091,DOI 10.1029/2001JD000892, 2002.

Creasey, D. J., Evans, G. E., Heard, D. E., and Lee, J. D.: Measurements of OH and HO_2 concentrations in the Southern Ocean marine boundary layer, J Geophys Res-Atmos, 108, 4475, Artn 4475, 10.1029/2002jd003206, 2003.

Ehhalt, D. H.: Photooxidation of trace gases in the troposphere Plenary Lecture, Physical Chemistry Chemical Physics, 1, 5401-5408, 10.1039/a905097c, 1999.

Emmerson, K. M., Carslaw, N., Carslaw, D. C., Lee, J. D., McFiggans, G., Bloss, W. J., Gravestock, T., Heard, D. E., Hopkins, J., Ingham, T., Pilling, M. J., Smith, S. C., Jacob, M., and Monks, P. S.: Free radical modelling studies during the UK TORCH Campaign in Summer 2003, Atmos Chem Phys, 7, 167-181, DOI 10.5194/acp-7-167-2007, 2007.

Fleming, Z. L., Monks, P. S., Rickard, A. R., Bandy, B. J., Brough, N., Green, T. J., Reeves, C. E., and Penkett, S. A.: Seasonal dependence of peroxy radical concentrations at a Northern hemisphere marine boundary layer site during summer and winter: evidence for radical activity in winter, Atmos. Chem. Phys., 6, 5415-5433, 10.5194/acp-6-5415-2006, 2006.

Forberich, O., Pfeiffer, T., Spiekermann, M., Walter, J., Comes, F. J., Grigonis, R., Clemitshaw, K. C., and Burgess, R. A.: Measurement of the Diurnal Variation of the OH Radical Concentration and Analysis of the Data by Modelling, Journal of Atmospheric Chemistry, 33, 155-181, 10.1023/A:1005973130335, 1999.

Furneaux, K. L.: Field Studies of the Chemistry of Free-Radicals in the Troposphere using Laser Induced Fluorescence Spectroscopy, PhD thesis, Ph.D., School of Chemistry, University of Leeds, Leeds, UK, available from https://library.leeds.ac.uk/info/1104/theses, 2009.

George, I. J., Matthews, P. S., Whalley, L. K., Brooks, B., Goddard, A., Baeza-Romero, M. T., and Heard, D. E.: Measurements of uptake coefficients for heterogeneous loss of HO_2 onto submicron inorganic salt aerosols, Phys Chem Chem Phys, 15, 12829-12845, 10.1039/c3cp51831k, 2013.

Green, T. J., Reeves, C. E., Fleming, Z. L., Brough, N., Rickard, A. R., Bandy, B. J., Monks, P. S., and Penkett, S. A.: An improved dual channel PERCA instrument for atmospheric measurements of peroxy radicals, Journal of environmental monitoring : JEM, 8, 530-536, 10.1039/b514630e, 2006.

Heard, D. E., Read, K. A., Methven, J., Al-Haider, S., Bloss, W. J., Johnson, G. P., Pilling, M. J., Seakins, P. W., Smith, S. C., Sommariva, R., Stanton, J. C., Still, T. J., Ingham, T., Brooks, B., De Leeuw, G., Jackson, A. V., McQuaid, J. B., Morgan, R., Smith, M. H., Carpenter, L. J., Carslaw, N., Hamilton, J., Hopkins, J. R., Lee, J. D., Lewis, A. C., Purvis, R. M., Wevill, D. J., Brough, N., Green, T., Mills, G., Penkett, S. A., Plane, J. M. C., Saiz-Lopez, A., Worton, D., Monks, P. S., Fleming, Z., Rickard, A. R., Alfarra, M. R., Allan, J. D., Bower, K., Coe, H., Cubison, M., Flynn, M., McFiggans, G., Gallagher, M., Norton, E. G., O'Dowd, C. D., Shillito, J., Topping, D., Vaughan, G., Williams, P., Bitter, M., Ball, S. M., Jones, R. L., Povey, I. M., O'Doherty, S., Simmonds, P. G., Allen, A., Kinnersley, R. P., Beddows, D. C. S., Dall'Osto, M., Harrison, R. M., Donovan, R. J., Heal, M. R., Jennings, S. G., Noone, C., and Spain, G.: The North Atlantic Marine Boundary Layer Experiment (NAMBLEX). Overview of the campaign held at Mace Head, Ireland, in summer 2002, Atmos Chem Phys, 6, 2241-2272, DOI 10.5194/acp-6-2241-2006, 2006.

Lakey, P. S. J.: Heteregeneous uptake of HO_2 radicals onto atmospheric aerosols, PhD thesis, School of Chemistry, University of Leeds, 2014.

Lakey, P. S., George, I. J., Whalley, L. K., Baeza-Romero, M. T., and Heard, D. E.: Measurements of the HO_2 uptake coefficients onto single component organic aerosols, Environ Sci Technol, 49, 4878-4885, 10.1021/acs.est.5b00948, 2015.

Lakey, P. S., George, I. J., Baeza-Romero, M. T., Whalley, L. K., and Heard, D. E.: Organics Substantially Reduce HO_2 Uptake onto Aerosols Containing Transition Metal ions, J Phys Chem A, 120, 1421-1430, 10.1021/acs.jpca.5b06316, 2016.

Lee, J. D., Young, J. C., Read, K. A., Hamilton, J. F., Hopkins, J. R., Lewis, A. C., Bandy, B. J., Davey, J., Edwards, P., Ingham, T., Self, D. E., Smith, S. C., Pilling, M. J., and Heard, D. E.: Measurement and calculation of OH reactivity at a United Kingdom coastal site, J Atmos Chem, 64, 53-76, 10.1007/s10874-010-9171-0, 2009.

Lu, K. D., Rohrer, F., Holland, F., Fuchs, H., Bohn, B., Brauers, T., Chang, C. C., Haseler, R., Hu, M., Kita, K., Kondo, Y., Li, X., Lou, S. R., Nehr, S., Shao, M., Zeng, L. M., Wahner, A., Zhang, Y. H., and Hofzumahaus, A.: Observation and modelling of OH and HO_2 concentrations in the Pearl River Delta 2006: a missing OH source in a VOC rich atmosphere, Atmos Chem Phys, 12, 1541-1569, 10.5194/acp-12-1541-2012, 2012.

Lu, K. D., Hofzumahaus, A., Holland, F., Bohn, B., Brauers, T., Fuchs, H., Hu, M., Häseler, R., Kita, K., Kondo, Y., Li, X., Lou, S. R., Oebel, A., Shao, M., Zeng, L. M., Wahner, A., Zhu, T., Zhang, Y. H., and Rohrer, F.: Missing OH source in a suburban environment near Beijing: observed and modelled OH and HO_2 concentrations in summer 2006, Atmos Chem Phys, 13, 1057-1080, 10.5194/acp-13-1057-2013, 2013.

Mao, J., Ren, X., Brune, W. H., Olson, J. R., Crawford, J. H., Fried, A., Huey, L. G., Cohen, R. C., Heikes, B., Singh, H. B., Blake, D. R., Sachse, G. W., Diskin, G. S., Hall, S. R., and Shetter, R. E.: Airborne measurement of OH reactivity during INTEX-B, Atmos Chem Phys, 9, 163-173, 10.5194/acp-9-163-2009, 2009.

Moon, D. R.: Heterogeneous reactions involving HO_2 radicals and atmospheric aerosols, PhD thesis, School of Chemistry, University of Leeds, available from White Rose E-theses online whiterose.ac.uk/20699, 2018.

Mozurkewich, M., McMurry, P. H., Gupta, A., and Calvert, J. G.: Mass Accommodation Coefficient for Ho2 Radicals on Aqueous Particles, J Geophys Res-Atmos, 92, 4163-4170, DOI 10.1029/JD092iD04p04163, 1987.

Osthoff, H. D., Roberts, J. M., Ravishankara, A. R., Williams, E. J., Lerner, B. M., Sommariva, R., Bates, T. S., Coffman, D., Quinn, P. K., Dibb, J. E., Stark, H., Burkholder, J. B., Talukdar, R. K., Meagher, J., Fehsenfeld, F. C., and Brown, S. S.: High levels of nitryl chloride in the polluted subtropical marine boundary layer, Nat Geosci, 1, 324-328, 10.1038/ngeo177, 2008.

Penkett, S. A., Clemitshaw, K. C., Savage, N. H., Burgess, R. A., Cardenas, L. M., Carpenter, L. J., McFadyen, G. G., and Cape, J. N.: Studies of oxidant production at the Weybourne Atmospheric Observatory in summer and winter conditions, Journal of Atmospheric Chemistry, 33, 111-128, Doi 10.1023/A:1005969204215, 1999.

Ravishankara, A. R.: Heterogeneous and multiphase chemistry in the troposphere, Science, 276, 1058-1065, DOI 10.1126/science.276.5315.1058, 1997.

Rohrer, F. and Berresheim, H.: Strong correlation between levels of tropospheric hydroxyl radicals and solar ultraviolet radiation, Nature, 442, 184-187, 10.1038/nature04924, 2006.

Salisbury, G., Rickard, A. R., Monks, P. S., Allan, B. J., Bauguitte, S., Penkett, S. A., Carslaw, N., Lewis, A. C., Creasey, D. J., Heard, D. E., Jacobs, P. J., and Lee, J. D.: Production of peroxy radicals at night via reactions of ozone and the nitrate radical in the marine boundary layer, Journal of Geophysical Research: Atmospheres, 106, 12669-12687, 10.1029/2000jd900754, 2001.

Sinha, V., Williams, J., Diesch, J. M., Drewnick, F., Martinez, M., Harder, H., Regelin, E., Kubistin, D., Bozem, H., Hosaynali-Beygi, Z., Fischer, H., Andres-Hernandez, M. D., Kartal, D., Adame, J. A., and Lelieveld, J.: Constraints on instantaneous ozone production rates and regimes during DOMINO derived using in-situ OH reactivity measurements, Atmos Chem Phys, 12, 7269-7283, 10.5194/acp-12-7269-2012, 2012.

Smith, S. C., Lee, J. D., Bloss, W. J., Johnson, G. P., Ingham, T., and Heard, D. E.: Concentrations of OH and HO_2 radicals during NAMBLEX: measurements and steady state analysis, Atmos Chem Phys, 6, 1435-1453, DOI 10.5194/acp-6-1435-2006, 2006.

Smith, S. C.: Atmospheric measurements of OH and HO_2 using the FAGE technique: Instrument development and data analysis, PhD thesis, School of Chemistry, University of Leeds, available from library.leeds.ac.uk/info/1104/theses, 2007.

Sommariva, R., Haggerstone, A.-L., Carpenter, L. J., Carslaw, N., Creasey, D. J., Heard, D. E., Lee, J. D., Lewis, A. C., Pilling, M. J., and Zádor, J.: OH and HO_2 chemistry in clean marine air during SOAPEX-2, Atmos. Chem. Phys., 4, 839–856, https://doi.org/10.5194/acp-4-839-2004, 2004.

Sommariva, R., Bloss, W. J., Brough, N., Carslaw, N., Flynn, M., Haggerstone, A. L., Heard, D. E., Hopkins, J. R., Lee, J. D., Lewis, A. C., McFiggans, G., Monks, P. S., Penkett, S. A., Pilling, M. J., Plane, J. M. C., Read, K. A., Saiz-Lopez, A., Rickard, A. R., and Williams, P. I.: OH and HO_2 chemistry during NAMBLEX: roles of oxygenates, halogen oxides and heterogeneous uptake, Atmos Chem Phys, 6, 1135-1153, DOI 10.5194/acp-6-1135-2006, 2006.

Sommariva, R., Bates, T. S., Bon, D., Brookes, D. M., de Gouw, J. A., Gilman, J. B., Herndon, S. C., Kuster, W. C., Lerner, B. M., Monks, P. S., Osthoff, H. D., Parker, A. E., Roberts, J. M., Tucker, S. C., Warneke, C., Williams, E. J., Zahniser, M. S., and Brown, S. S.: Modelled and measured concentrations of peroxy radicals and nitrate radical in the U.S. Gulf Coast region during TexAQS 006, Journal of Atmospheric Chemistry, 68, 331-362, 10.1007/s10874-012-9224-7, 2011.

Sommariva, R., Hollis, L., Sherwen, T., R Baker, A., M Ball, S., J Bandy, B., G Bell, T., N Chowdhury, M., Cordell, R., Evans, M., D Lee, J., Reed, C., E Reeves, C., M Roberts, J., Yang, M., and Monks, P.: Seasonal and geographical variability of nitryl chloride and its precursors in Northern Europe, e844 pp., 10.1002/asl.844, 2018.

Stone, D., Whalley, L. K., and Heard, D. E.: Tropospheric OH and HO_2 radicals: field measurements and model comparisons, Chem Soc Rev, 41, 6348-6404, 10.1039/c2cs35140d, 2012.

Tan, Z. F., Fuchs, H., Lu, K. D., Hofzumahaus, A., Bohn, B., Broch, S., Dong, H. B., Gomm, S., Haseler, R., He, L. Y., Holland, F., Li, X., Liu, Y., Lu, S. H., Rohrer, F., Shao, M., Wang, B. L., Wang, M., Wu, Y. S., Zeng, L. M., Zhang, Y. S., Wahner, A., and Zhang, Y. H.: Radical chemistry at a rural site (Wangdu) in the North China Plain: observation and model calculations of OH, HO_2 and RO_2 radicals, Atmos Chem Phys, 17, 663-690, 10.5194/acp-17-663-2017, 2017.

Tan, Z. F., Rohrer, F., Lu, K. D., Ma, X. F., Bohn, B., Broch, S., Dong, H. B., Fuchs, H., Gkatzelis, G. I., Hofzumahaus, A., Holland, F., Li, X., Liu, Y., Liu, Y. H., Novelli, A., Shao, M., Wang, H. C., Wu, Y. S., Zeng, L. M., Hu, M., Kiendler-Scharr, A., Wahner, A., and Zhang, Y. H.: Wintertime photochemistry in Beijing: observations of RO_x radical concentrations in the North China Plain during the BEST-ONE campaign, Atmos Chem Phys, 18, 12391-12411, 10.5194/acp-18-12391-2018, 2018.

Thames, A. B., Brune, W. H., Miller, D. O., Allen, H. M., Apel, E. C., Blake, D. R., Bui, T. P., Commane, R., Crounse, J. D., Daube, B. C., Diskin, G. S., DiGangi, J. P., Elkins, J. W., Hall, S. R., Hanisco, T. F., Hannun, R. A., Hintsa, E., Hornbrook, R. S., Kim, M. J., McKain, K., Moore, F. L., Nicely, J. M., Peischl, J., Ryerson, T. B., St. Clair, J. M., Sweeney, C., Teng, A., Thompson, C. R., Ullmann, K., Wennberg, P. O., and Wolfe, G. M.: Missing OH reactivity in the global marine boundary layer, Atmos. Chem. Phys., 20, 4013-4029, 10.5194/acp-20-4013-2020, 2020.

van Stratum, B. J. H., Vilà-Guerau de Arellano, J., Ouwersloot, H. G., van den Dries, K., van Laar, T. W., Martinez, M., Lelieveld, J., Diesch, J. M., Drewnick, F., Fischer, H., Hosaynali Beygi, Z., Harder, H., Regelin, E., Sinha, V., Adame, J. A., Sörgel, M., Sander, R., Bozem, H., Song, W., Williams, J., and Yassaa, N.: Case study of the diurnal variability of chemically active species with respect to boundary layer dynamics during DOMINO, Atmos Chem Phys, 12, 5329-5341, 10.5194/acp-12-5329-2012, 2012.

Vaughan, S., Ingham, T., Whalley, L. K., Stone, D., Evans, M. J., Read, K. A., Lee, J. D., Moller, S. J., Carpenter, L. J., Lewis, A. C., Fleming, Z. L., and Heard, D. E.: Seasonal observations of OH and HO_2 in the remote tropical marine boundary layer, Atmos Chem Phys, 12, 2149-2172, 10.5194/acp-12-2149-2012, 2012.

Whalley, L. K., Furneaux, K. L., Goddard, A., Lee, J. D., Mahajan, A., Oetjen, H., Read, K. A., Kaaden, N., Carpenter, L. J., Lewis, A. C., Plane, J. M. C., Saltzman, E. S., Wiedensohler, A., and Heard, D. E.: The chemistry of OH and HO_2 radicals in the boundary layer over the tropical Atlantic Ocean, Atmos Chem Phys, 10, 1555-1576, 10.5194/acp-10-1555-2010, 2010

Zannoni, N., Gros, V., Esteve, R. S., Kalogridis, C., Michoud, V., Dusanter, S., Sauvage, S., Locoge, N., Colomb, A., and Bonsang, B.: Summertime OH reactivity from a receptor coastal site in the Mediterranean Basin, Atmos Chem Phys, 17, 12645-12658, 10.5194/acp-17-12645-2017, 2017.

..